Optics Letters

Aspheric lens to increase the depth of focus

Alexis Vázquez-Villa,[1,*] José A. Delgado-Atencio,[2] Sergio Vázquez-Montiel,[2] Jorge Castro-Ramos,[1] and Margarita Cunill-Rodríguez[2]

[1]Instituto Nacional de Astrofísica Óptica y Electrónica, Luis Enrique Erro #1, Tonantzintla, Puebla C.P. 72840, Mexico
[2]Cuerpo Académico de Computación Óptica, Universidad Politécnica de Tulancingo. Calle Ingenierías No. 100, Huapalcalco, Hidalgo, Mexico
*Corresponding author: vazquezvilla@gmail.com

For high-resolution optical systems, a long depth of focus is desirable. Unfortunately, resolution and depth of focus are inversely related. In this work, a novel lens is presented to produce long depth of focus beams, keeping the same resolution. The equations to perform the optical design of this kind of lenses and results are shown for a simple lens that can produce beams with a spot size of 2.9 μm over a range of 1.5 mm and for an achromatic doublet with a focus depth of 10 mm. © 2015 Optical Society of America

High-resolution optical systems like OCT [1,2], two photon microscopy [3], and optical micromanipulation [4], among others, require simultaneously high resolution (spot size) and extended depth of focus. Unfortunately, the depth of focus (DOF) and the resolution are inversely related (e.g., in Gaussian beams), by two times the Rayleigh distance [5] Z_R, meaning that an increment in resolution will result in a decrement of the depth of focus:

$$2Z_R = \frac{8\lambda f^2}{\pi D^2}, \qquad (1)$$

where λ is the wavelength, f is the focal length of the optical system, and D is the spot size in the lens.

Several approaches to solve this issue have been attempted by different groups such as the use of dynamic focus [6–10] with the downside of increased imaging time, and the use of computational algorithms [11,12] to correct images out of focus with the disadvantage of higher computational power. Also the use of conical refractive surfaces to generate Bessel beams has been applied [13–15]. Another similar approach is the use of spatial light modulator (SLM) [16,17] to generate non-diffraction beams, but SLM are expensive and difficult to implement in optical systems. The method we are presenting is similar to the so-called Conrady's D-d method of achromatization of a lens where the radius of the last surface is found in order to satisfy Conrady's condition [18]. However, in our method, aspheric coefficients of the last surface are calculated in order to find a range along the z-axis where the size of light beam and its irradiance are relatively steady.

In this work, a novel type of lense is presented that can produce a long depth of focus. The concept is based on the research work reported by Vázquez and Garcia [19] consisting of an analytic method to correct the spherical aberration using exact ray tracing and an aspherical surface. In this case, instead of correcting the spherical aberration, the aspherical surface is used to produce a zone with low change in intensity and spot size. The method involves calculating the aspheric coefficients for the surface (e.g., the last area) equaling the optical path of a ray coming from a specific height in the entrance pupil with the optical path of a ray through the center of the entrance pupil along the optical axis.

Considering that the aspherical surface has rotational symmetry, the meridional plane was used to define the surface and using a ray with a specific height y_0 at the entrance pupil. The sag of the aspherical surface $Z_{\text{aspheric(height)}}$ in the last surface is expressed as [19]

$$z_{\text{aspheric(height)}} = z_{\text{spheric(height)}} + a_1(y_{k-1(\text{height})})^4$$
$$+ a_2(y_{k-1(\text{height})})^6 + \ldots + a_n(y_{k-1(\text{height})})^{2n}, \qquad (2)$$

where $Z_{\text{spheric(height)}}$ is the sag of the spherical surface in the last surface, and y_{k-1} is the height on the last surface being both of them calculated using exact ray tracing. Rays with different heights on the entrance pupil are used to calculate more than one aspheric coefficient, for example, using five-rays at different heights, five coefficients of the Eq. (2) are obtained. Then it is more adequate and advantageous to formulate Eq. (2) in matrix form:

$$
\begin{bmatrix} c_1 \\ c_2 \\ c_3 \\ c_4 \\ \vdots \\ c_n \end{bmatrix}
=
\begin{bmatrix}
b_{11} & b_{21} & b_{31} & b_{41} & \cdots & b_{n1} \\
b_{12} & b_{22} & b_{32} & b_{42} & \cdots & b_{n2} \\
b_{13} & b_{23} & b_{33} & b_{43} & \cdots & b_{n3} \\
b_{14} & b_{24} & b_{34} & b_{44} & \cdots & b_{n4} \\
\vdots & \vdots & \vdots & \vdots & \vdots & \vdots \\
b_{1n} & b_{2n} & b_{3n} & b_{4n} & \cdots & b_{nn}
\end{bmatrix}
\begin{bmatrix} a_1 \\ a_2 \\ a_3 \\ a_4 \\ \vdots \\ a_n \end{bmatrix}, \qquad (3)
$$

where $c_{1,2,3,\ldots,n}$ are the difference $z_{\text{aspheric}} - z_{\text{spheric}}$, $b_{11,12,\ldots,nn}$ are the coordinates on the last surface for the ray to the fourth,

sixth, octave, etc. power, and $a_{1,2,...,n}$ are the aspheric coefficients of the aspherical surface.

The coordinates before the last surface are calculated using exact ray tracing, the coordinates of the ray in the last surface are

$$y_{k-1} = y_{k-2} + D_{k-1}M_{k-1}, \tag{4}$$

$$z_{\text{aspheric}} = z_{k-1} = z_{k-2} - d_{k-1} + D_{k-1}N_{k-1}, \tag{5}$$

$$z_{\text{spheric}} = \frac{c_{k-1}y_{k-1}^2}{1 + \sqrt{1 - c_{k-1}^2 y_{k-1}^2}}, \tag{6}$$

where y_{k-2} and z_{k-2} are the coordinates on the penultimate surface, M_{k-1} and N_{k-1} are the direction cosines of the ray in the same surface, and d_{k-1} is the distance along the optical axis between the last and the previous surface. All the former parameters can be calculated using exact ray tracing for $k-1$ surfaces previous to the aspherical surface (see Fig. 1). The parameter D_k is the distance along the ray path to a desire distance d_k in the optical axes and it is calculated as follows:

$$D_k = \sqrt{(y_{k-2} + M_{k-1}D_{k-1})^2 + (d_k - z_{k-2} + d_{k-1} - N_{k-1}D_{k-1})^2}. \tag{7}$$

To calculate D_{k-1} is necessary to solve the following quadratic equation:

$$AD_{k-1}^2 + BD_{k-1} + C = 0. \tag{8}$$

If the object is at infinity, A, B, and C are calculated as

$$A = n_k^2 - n_{k-1}^2, \tag{9}$$

$$B = 2 \begin{bmatrix} n_k^2 y_{k-1}M_{k-1} - n_k^2 N_{k-1}(d_k - z_{k-1} + d_{k-1}) \\ +n_{k-1}(n_1 d_1 + ... + n_{k-1}d_{k-1} + n_k d_k) \\ -n_1 D_1 - ... - n_{k-2}D_{k-2} - n_0 z_1) \end{bmatrix}, \tag{10}$$

$$C = \begin{bmatrix} n_k^2 y_{k-1}^2 + n_k^2 (d_k - z_{k-1} + d_{k-1})^2 \\ -(n_1 d_1 + ... + n_{k-1}d_{k-1} + n_k d_k) \\ -n_1 D_1 - ... - n_{k-2}D_{k-2} - n_0 z_1)^2 \end{bmatrix}. \tag{11}$$

Then the coordinates on the last surface are calculated, and the equation system (3) is solved to obtain the aspherical coefficients contained in the vector a.
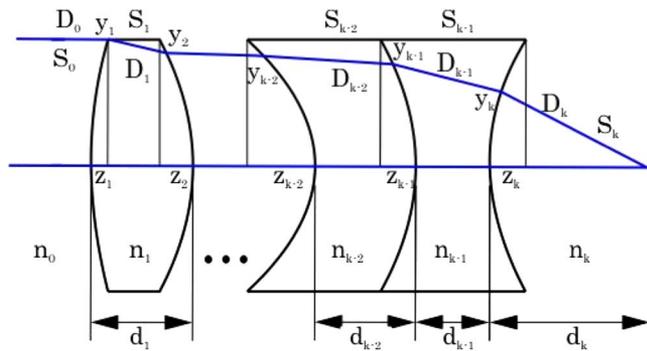

Fig. 1. Parameters used for calculating the coefficients of the aspherical surface. $D_{0,1,...,k}$ are the distances along the ray path, $n_{0,1,...,k}$ are the refractive indices of each medium, $d_{0,1,...,k}$ are the distances along the optical axis between surfaces, $S_{0,1,...,k}$ are the ray (direction cosines), $y_{0,1,...,k-1}$ and finally $z_{0,1,...,k-1}$ are the coordinates of the ray for each surface.

To generate beams with long depth of focus, rather than equal to the optical path of the edge and zonal rays with the paraxial ray, the rays were directed to different points on the optical axes using different sections of the lens. For example, Fig. 2 shows the Zemax layout for a lens illuminated using collimated light. In Fig. 2(a), the lens has two different focal points because of the spherical aberration, for this lens, the edge rays focus before the back focal length (BFL). In Fig. 2(b), the aspherical surface also has two focal points, but instead of the spherical case, it sends the edge rays at a desire distance d_k of the BFL. The focal points are chosen using different distances d_k for different zonal rays of the lens. The distances must be chosen in a manner that a volume with a constant spot size is generated along the optical axis. In order to have a similar f-number for the two focal points, the edge rays must focus after the BFL to produce a zone where the spot size and intensity remains practically constant.

As a simple example of the above outlined method, a plano-convex lens is presented; the parameters of this lens are summarized in Table 1. The HPSF (Huygens point spread function) was calculated at different image distances for the normal plano-convex lens and for the aspheric lens using the flat surface as the aspheric surface. The simulation used a central wavelength of $\lambda = 587.56$ nm, the entrance pupil diameter is 25.4 mm, and the effective focal length is 50 mm. One aspherical coefficient was used to generate the aspherical surface. A height of $y_0 = 12.70$ mm and the distance $d_k = 1$ mm were used to calculate the aspherical coefficient, resulting for it the value $a_1 = 8.1154 \times 10^{-6}$ mm^{-3}.

In Figs. 3(d) and 3(f), the HPSFs remain similar in shape and also in their relative intensity. The distance between these two points is of one millimeter. Also, the HPSF shape is similar to a Bessel beam with an intense central spot surrounded by rings of less intensity. Figure 4(a) and 4(b) shows the HPSF cross-section for the distances of 0.7 mm and 2 mm, respectively, after BFL. Figure 4(c) shows the changes for the FHWM and relative intensity between the ranges of 0.6–2.1 mm after the BFL. For this range, the mean FWHM is 1.05 ± 0.31 µm, and
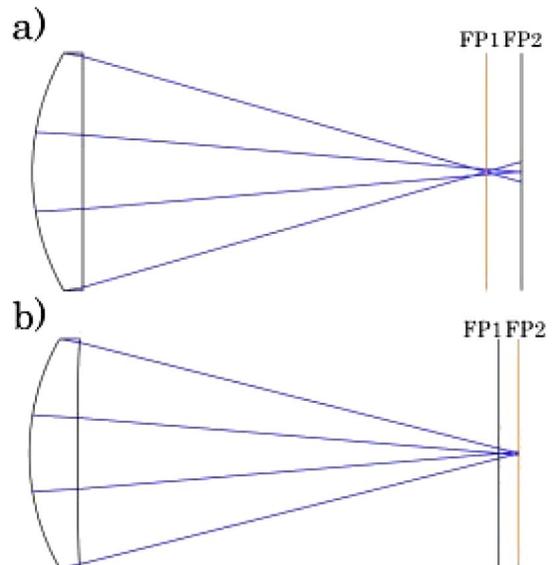

Fig. 2. Plano-convex lens, (a) normal spherical lens, (b) aspherical lens. Both lenses are illuminated using collimated light.

Table 1. Parameters of Plano-Convex Lens

Surface	Radius [mm]	Thickness [mm]	Semi-Diameter [mm]	Material	Height [mm]	Coefficient
Object		Infinity		Air	12.70	$a_1 = 8.1154 \times 10^{-6}$ mm^{-3}
1	25.840	5.340	12.70	BK7		
2	Infinity	46.479	12.70	Air		
Image				Air		

the mean relative irradiance is $8.24 \times 10^{-3} \pm 2.79 \times 10^{-3}$ W/mm^2. The airy disk radius for this lens is 1.458 µm. Because the calculated FWHM is below the airy disk, we could consider the spot size to remain in the same range and the DOF = 1.5 mm. For the spherical lens, the maximum relative intensity is 1×10^{-3} W/mm^2, and the calculated depth of focus DOF = 5.8 µm was obtained from Eq. (1). This means that the DOF is increased almost 260 times.

Finally, another important aspect to be considered regarding this finding is the degree of difficulty to fabricate the aspherical surface. Essentially, in this example, fabricating the lens will not be so complicated due to the following factors: (1) one surface is a spherical surface, (2) only one aspherical coefficient was
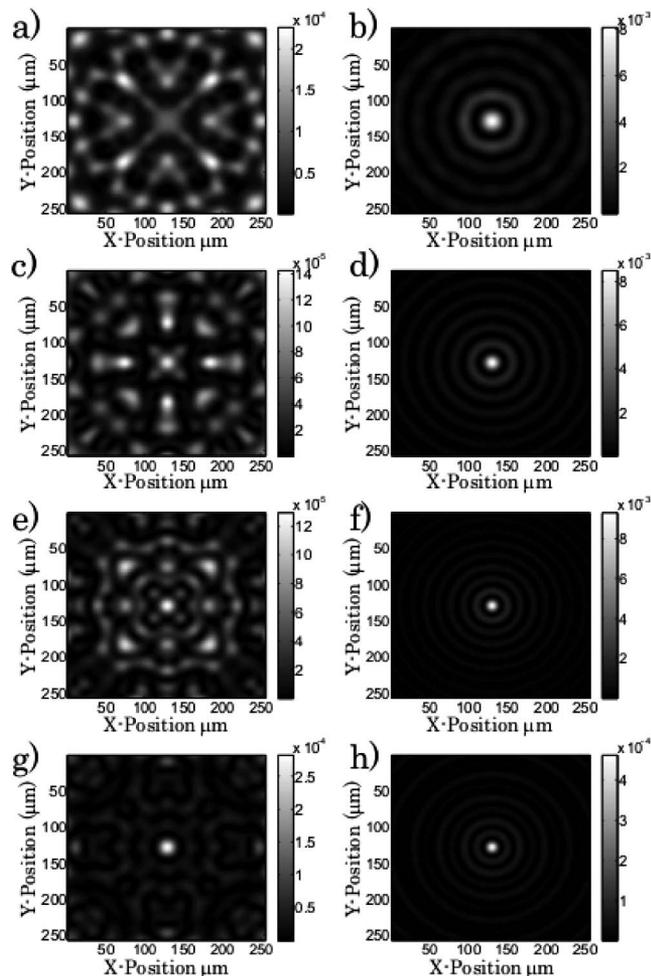
Fig. 4.   (a),(b) show HPSF cross-section for the distance 0.7 mm and 2.0 mm after BFL. (c) shows FHWM (solid line) and relative irradiance (dashed line) changes between the ranges of 0.6 mm to 2.1 mm.

needed to the aspherical surface, and (3) both surfaces have revolution symmetry (see Fig. 5) making the lens not so complicated to manufacture. Of course, for another type of aspherical surface (e.g., using more aspherical coefficients), the surface could become much more complex to fabricate.

As a second example to show the versatility of our method, we design an achromatic doublet and calculate four coefficients

Fig. 3.   Huygens point spread functions (HPSFs) for spherical lens are shown in the left column whereas for the aspherical lens are shown in the right column. The variable parameter along the rows is the distance from the last surface of the lens to: (a) and (b) 0.5 mm, (c) and (d) 1 mm, (e) and (f) 2 mm, and (g) and (h) 2.3 mm.
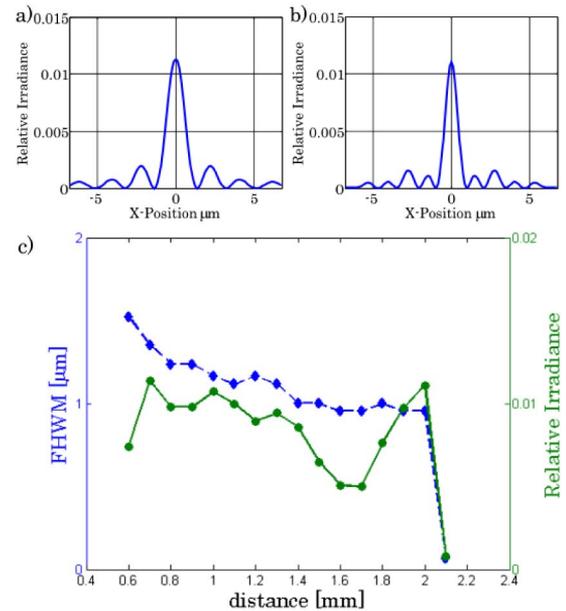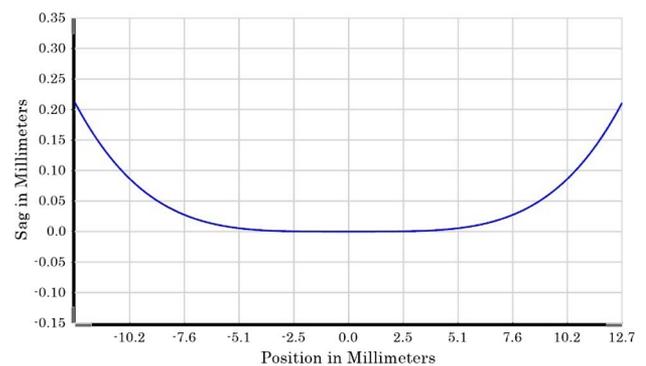
Fig. 5.   Surface sagittal cross-section for the aspherical surface of the designed lens. Because it was designed from a flat surface, the center part of the lens remains flat and only in the borders is created a curvature.

Table 2. Parameters of Achromatic Doublet

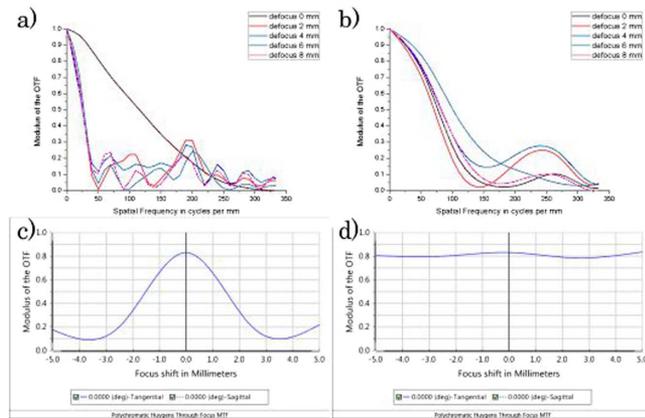| Surface	Radius [mm]	Thickness [mm]	Semi-Diameter [mm]	Material	Height [mm]	Coefficient
Object		Infinity		Air	5.0	$a_1 = 1.851534 \times 10^{-4}$ mm^{-3}
1	30.7482	2.00	5	BK7	4.0	$a_2 = -5.787789 \times 10^{-5}$ mm^{-5}
2	−22.4844	1.00	5	SF5	2.0	$a_3 = 5.221834 \times 10^{-6}$ mm^{-7}
3	−65.5561	50.00	5	Air	1.0	$a_4 = -1.274732 \times 10^{-7}$ mm^{-9}
Image				Air		

Fig. 6. (a) and (c) containing the calculated MTF for five different positions of the image plane and the MTF through focus on a range of 10 mm for conventional doublet. (b) and (d) are the calculated MTF for five positions of the image plane and the MTF through focus on a range of 10 mm for the doublet with the aspheric surface.

of asphericity using four rays at different heights in the entrance pupil obtaining a depth of focus of 10 mm. Table 2 shows the construction parameters of the doublet and the coefficients of asphericity. In Fig. 6, you can see a performance comparison between the conventional doublet and the doublet with the aspherical surface. In the left column appears the MTF for five different positions of the image plane and the MTF through focus in a range of 10 mm, and in the right column appears the same but for the doublet with the aspherical surface. As can be seen, the MTF through focus remains virtually constant when changing the position of the image plane, thereby the robustness of our method is demonstrated.

In conclusion, it has been demonstrated that using this methodology, it is feasible to design a lens with an extended depth of focus. In addition, it is possible to define the distance between the two focal points, and if this distance is below the original spherical aberration, then the relative intensity is increased. Furthermore the design method allows using n number of surfaces because it requires only modifying the last surface, and then more complex lenses can be used to correct other aberrations, for example, chromatic aberration, and produce long depth of focus beams. Finally, an aspherical surface could be easier to fabricate and will have a lower cost than the option of using and fabricating an axicon that has a conical surface that increases the manufacture costs.

REFERENCES

1. W. Drexler, U. Morgner, F. X. Kärtner, C. Pitris, S. A. Boppart, X. D. Li, E. P. Ippen, and J. G. Fujimoto, Opt. Lett. **24**, 1221 (1999).
2. W. Drexler, J. Bio. Opt. **9**, 47 (2004).
3. P. Dufor, M. Piché, Y. D. Koninck, and N. McCarthy, Appl. Opt. **45**, 36 (2006).
4. J. Arlt, V. Garces-Chavez, W. Sibbett, and K. Dholakia, Opt. Commun. **197**, 239 (2001).
5. W. Drexler, Y. Chen, A. Aguirre, B. Povazay, A. Unterhuber, and J. G. Fujimoto, *Optical Coherence Tomography Technology and Applications*, W. Drexler and J. G. Fujimoto, eds. (Springer, 2008). pp. 239–279.
6. M. Subbarao and J. Tyan, IEEE Trans. Pattern Anal. Mach. Intell. **20**, 864 (1998).
7. F. Lexer, C. K. Hitzenberg, W. Drexler, S. Molebny, H. Sattmann, M. Sticker, and A. F. Fercher, J. Mod. Opt. **46**, 541 (1999).
8. B. Qi, A. P. Himmer, L. M. Gordon, X. D. V. Yang, L. D. Dickensheets, and I. A. Vitkin, Opt. Commun. **232**, 123 (2004).
9. P. Meemon, K. Lee, S. Murali, and J. Rolland, Appl. Opt. **47**, 2452 (2008).
10. A. D. Aguirre, J. Sawinski, S. Huang, C. Zhou, W. Denk, and J. G. Fujimoto, Opt. Express **18**, 4222 (2010).
11. A. G. Valdecasas, D. Marshall, J. M. Becerra, and J. J. Terrero, Micron **32**, 559 (2001).
12. P. S. Carney and S. A. Boppart, "Advanced OCT/computed imaging: Depth of field and resolution meet in new OCT approach," in Bio Optics World (2011), http://www.biopticsworld.com/articles/print/volume-4/issue-2/optical-coherence-tomography/advanced-oct-computed-imaging-depth-of-field-and-resolution-meet-in-new-oct-approach.html.
13. Z. Ding, H. Ren, Y. Zhao, J. S. Nelson, and Z. Chen, Opt. Lett. **27**, 243 (2002).
14. R. A. Leitgeb, M. Villiger, A. H. Bachmann, L. Steinmann, and T. Lasser, Opt. Lett. **31**, 2450 (2006).
15. K. Lee and J. P. Rolland, Opt. Lett. **33**, 15 (2008).
16. N. Davidson, A. A. Friesem, and E. Hasman, Opt. Lett. **16**, 7 (1991).
17. C. Iemmi, J. Campos, J. C. Escalera, O. Lopez-Coronado, R. Gimeno, and M. J. Yzuel, Opt. Express **14**, 22 (2006).
18. A. E. Conrady, Mon. Not. R. Astron. Soc. **64**, 182 (1904).
19. S. Vazquez-Montiel and O. Garcia-Lievanos, Rev. Mex. Fis. **59**, 273 (2013).